

# Investigating the use of Symbol Timing Recovery for Medium-Derived Feedback in Nanopositioning Controllers

Andreas Kotsopoulos and Theodore Antonakopoulos

**Abstract**—Accurate nanopositioning is of significant importance in modern Atomic Force Microscopy (AFM) applications that demand high-speed and ultra-precise probe operation. In such applications, position sensors are mostly used in order to provide the control mechanism with feedback regarding probe movement. It has been shown experimentally that the measurement noise introduced by the positioning sensors significantly impairs the overall system performance. In this work, the use of symbol timing recovery for providing medium-derived velocity feedback in nanopositioning tracking controllers for probe-based storage devices is investigated. Although dedicated storage areas with predefined data sequences are used to provide real-time estimates of the system velocity, the proposed approach can also be applied to systems using non-data aided symbol timing recovery. A complete controller enhanced with timing synchronization feedback was designed and its performance was evaluated. It is shown that this medium-derived velocity estimation can be used as an alternative to the sensor-derived position or velocity readings with similar and in some cases superior performance results for a given motion controller. The superiority of the proposed scheme is even more profound when controllers of high-speed nanopositioning are considered, due to the elimination of the position sensor measurement noise, which would corrupt the usually used high-bandwidth closed loop system.

## I. INTRODUCTION

Driven by the wide range of Atomic Force Microscopy (AFM) and Scanning Probe Microscopy (SPM) based nanoscale science and technology applications, such as imaging, nanofabrication and probe-based data storage [1], [2], [3], the need of efficient nanopositioning is constantly growing in order to meet the emerging requirements for both high-speed and precise operation. In probe-based data storage systems, Micro-Electro-Mechanical-System (MEMS) or piezoelectric (PZT) actuated nanopositioning scanners [4] with x/y-axis displacement capabilities are used to properly displace an array of probes with respect to the storage medium plane (or usually vice versa) along the desired trajectory [1], [5] during read, write and erase data operations. These operations are carried out by specially manufactured micro-cantilever probes, with the capability to sense and alter the status of the storage medium's properties depending on the technology, together with appropriate readback circuitries and signal processing units lying behind the probes.

Feedback is typically provided to the underlying motion control mechanism by position sensors mounted on the scanner. The quality of the available feedback information plays a key role to the overall achieved precision. During the

scan operation, the scanner undergoes perturbations caused by noise sources and disturbances of diverse nature and frequency range. In shock and vibration protected environments, external disturbances can be considered to have a negligible effect on the scanner motion. In this case these perturbations are mainly due to the measurement noise introduced by the sensor and are a significant source of timing error in the readback signal [6]. Moreover, high-speed nanopositioning schemes, in principle result in systems with higher closed loop bandwidths and, in consequence, with increased susceptibility to measurement noise [7].

In this paper, we investigate the use of symbol timing recovery (STR) techniques in order to provide medium-derived velocity feedback in nanopositioning tracking controllers for probe storage devices, instead of, or auxiliary to the standard position feedback information provided by the positioning sensors. Medium-derived velocity feedback can be achieved by exploiting the readback signal samples and the usually used symbol timing recovery loop to extract an estimate of system's velocity. The data samples are provided by synchronization-dedicated probes, which act upon special storage medium regions with pre-stored and a priori known preamble symbol sequences. Although dedicated storage areas with predefined data sequences are used to provide real-time estimates of the system velocity, the proposed approach can also be applied to systems using non-data aided symbol timing recovery. Read, write and erase storage operations are carried out, while the medium is properly displaced with respect to the cantilever, usually along a raster or a similar pattern. In the context of this work, it is assumed that the system does not deviate from the center of the scanned track in the y direction, and hence, in the analysis that follows only operations on a single track along the x-axis are considered.

The advantages of such an approach for a probe-based storage device are the following. Firstly, the medium-derived information is less sensitive to some of the noise sources corrupting position sensor readings, such as ambient electrical, and can hence provide higher sensing resolution in many cases. Secondly, it enhances the fault-tolerance properties of the overall device, since position sensors are no longer the system's single-point-of-failure. In case of sensor unavailability, similar tracking performance could be achieved using the medium-derived feedback path. Moreover, the use of readback signal robustifies the device's data detection and overall bit-error rate properties against possible storage-medium contractions and expansions stemming from environmental factors such as changes in temperature and medium expansion. This type of very low frequency

The authors are with the Department of Electrical and Computers Engineering, University of Patras, 26500 Rio - Patras, Greece. akotsop, antonako@upatras.gr

disturbance affects the actual distance between successive stored symbols and is invisible to the control mechanism. This problem cannot be ultimately addressed by the synchronization loop alone, because of the latter's limited lock range. This motivates a joint control-synchronization system, able to detect and cope with such physical changes in the system. Furthermore, it enables the use of cost-effective solutions for the position sensors and ADCs, which can be used only for coarse initial position or velocity establishment. Finally, switching off the position sensors, the respective ADCs and relative circuitry during tracking can lead to decreased power consumption, which is an essential factor, especially if a mobile storage device is considered.

In Section II, the positioning system under consideration is described. Section III presents the architecture of the overall system as well as the design of the controller and the timing synchronization loop. Finally, Section IV analyzes the performance results and advantages of the proposed architecture.

## II. SCANNER IDENTIFICATION AND MODELING

The control mechanisms presented in this work were developed for a model of a scanning-probe data storage experimental setup with thermomechanical and optical read and thermomechanical write capabilities. Information is stored as sequences of indentations written on thin polymer films using an AFM cantilever. Thermomechanical writing is performed by applying an electrostatic force to the polymer layer and simultaneously softening the polymer layer by local heating. Readback is achieved by measuring the thermal conductance between the probe and the storage substrate or the deflection of a laser beam due to the cantilever's displacement. The presence or the absence of indentations corresponds to logical 1s or 0s, respectively.

The nanopositioning system is based on a piezoelectrically actuated scanner, capable of displacing the storage medium with respect to the cantilever tip in the  $x$ ,  $y$  and  $z$  axis. Position feedback in the  $x/y$  plane is provided by two capacitive sensors one for each direction of motion and two 18-bit Analog-to-Digital Converters (ADCs). The measured power spectral density (PSD) of the combined noise is presented in Fig. 1 for the  $x$ -axis sensor, showing the relatively high spectral components at the odd multiples of 50 Hz due to ambient electrical noise.

The experimentally obtained frequency response in the  $x$  direction is depicted in Fig. 2, together with the corresponding sixth-order transfer function fit. The reduced model captures well the first two resonances of the plant and was used for the  $H_\infty$  controller synthesis process, while the simulations were carried out with a higher order model. The scanner presents an almost flat response until the first resonances, which appear at 374 Hz in the  $x$  axis. However, the delay introduced by the high charge/discharge time constants of the capacitive elements (due to the supported long travel ranges) result in high phase loss and limit the achievable closed-loop bandwidth.

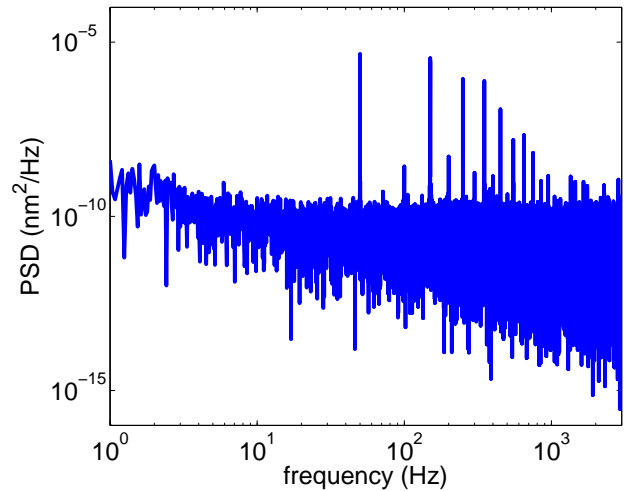


Fig. 1. Measured capacitive sensor noise power spectral density.

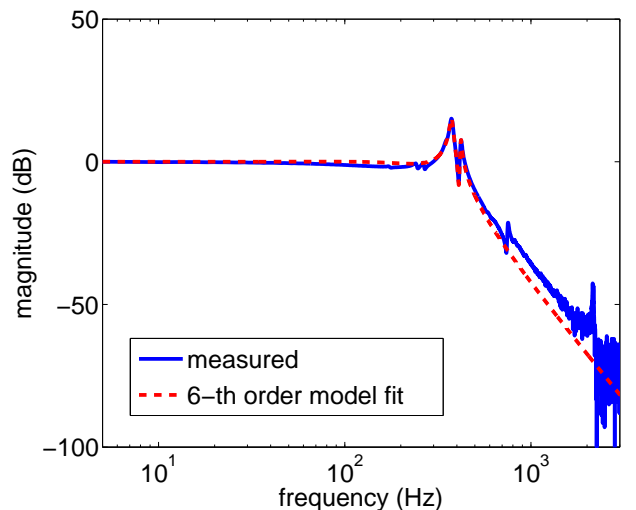


Fig. 2. Experimentally obtained  $x$ -axis scanner frequency response.

## III. SYSTEM ARCHITECTURE

The block diagram of the proposed control architecture of the overall system is shown in Fig. 3. The first-order loop comprises an  $H_\infty$  controller denoted by  $K_{H_\infty}$ , and a cascaded notch filter denoted by  $K_{NF}$  to compensate for the unmodeled higher order resonances. Instead of using the integrated sensor to provide position feedback to the controller, feedback is provided by a non-synchronous first-order symbol timing recovery loop, which is used to calculate an estimate of the scanner's current linear velocity. From this estimate the velocity error signal is extracted, which is fed back to the  $H_\infty$  tracking controller after appropriate transformation. Maintaining a constant linear velocity is a matter of major significance in probe-based data storage, since fixed-spaced sampling and constant oversampling are required for proper execution of data operations and data detection.

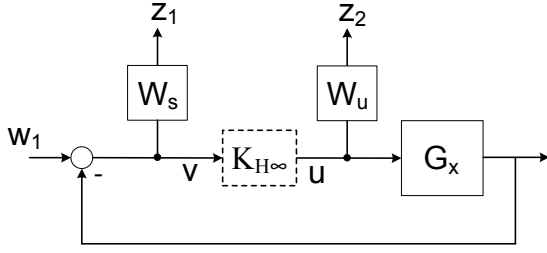


Fig. 4.  $H_\infty$  control design problem formulation.

The proposed architecture implies that the system moves on or very close to the center of the track, where the synchronization pattern is stored. This is achieved by the y-axis tracking controller and is outside the scope of this work. Various y-axis tracking controllers for raster scanning in probe storage have been studied in the literature, using sensors and/or medium-derived positioning error signal techniques [4], [8]. In the subsections that follow, the  $H_\infty$  controller and the STR loop design are separately presented.

#### A. $H_\infty$ Controller Design

The  $H_\infty$  problem formulation is shown in Fig. 4. The sixth-order transfer function fit produced an eighth-order controller, resulting in a closed loop system of approximately 40 Hz bandwidth. The shaping specifications for the closed loop transfer functions were captured by the weighting functions  $W_s$  and  $W_u$  shown in Fig. 5, expressing the requirements on tracking performance and control effort limits respectively. Finally,  $v$  and  $u$  denote the input to the controller and the controlled output respectively, while  $w = [w_1]$  the “exogenous input” signal vector and  $z = \begin{bmatrix} z_1 \\ z_2 \end{bmatrix}$  the “exogenous output” signal vectors.

The system can then be described as:

$$\begin{bmatrix} z_1 \\ z_2 \\ v \end{bmatrix} = P \cdot \begin{bmatrix} w_1 \\ u \end{bmatrix}, \quad u = K_{H_\infty} v \quad (1)$$

where  $P$  denotes the generalized plant given by:

$$P = \begin{bmatrix} W_s & -W_s G_x \\ 0 & W_u \\ 1 & -G_x \end{bmatrix} \quad (2)$$

The closed loop transfer function matrix  $T_{zw}$  relating  $z$  with  $w$  is the linear fractional transformation of  $K_{H_\infty}$  around  $P$ , given by:

$$T_{zw} = F_l(P, K) = \begin{bmatrix} \frac{W_s}{1+G_x K_{H_\infty}} \\ \frac{W_u K_{H_\infty}}{1+G_x K_{H_\infty}} \end{bmatrix} \quad (3)$$

#### B. Symbol Timing Recovery Loop Design

The architecture of the STR loop is depicted in the block diagram of Fig. 3. While the probe is scanned along the specified track, data samples from a synchronization-dedicated medium region are available at the input of the STR with a

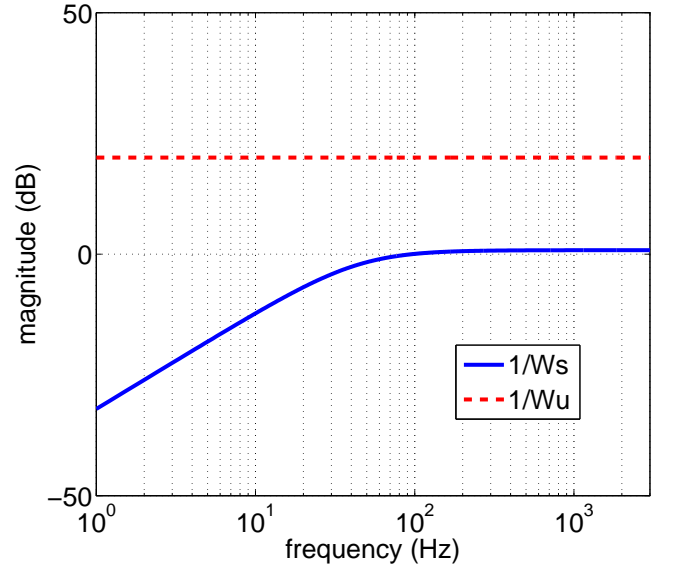


Fig. 5. Performance and control input weighting transfer functions.

fixed rate of  $1/T_s$  through the readback path circuitry and a dedicated 18-bit ADC. A prestored preamble synchronization pulse train is assumed, consisting of a repeating “0 1” logical symbol pattern of symbol pulses similar to raised cosine pulses.

The loop is based on a Gardner timing error detector (TED) [9], [10], [11], which uses two samples per symbol in order to produce timing error signal samples  $e_{TED}$  at symbol rate. Given the reference constant linear velocity  $v_{rx}$  and a spatial intersymbol distance  $B_P$ , the nominal symbol rate can be readily expressed as  $F = v_{rx}/B_P$ . The estimated timing error for the  $k$ -th symbol is calculated by:

$$e_{TED_k} = y[kT - T/2](y[(k-1)T] - y[kT]) \quad (4)$$

where  $y[\cdot]$  denotes the cubic interpolator output samples. The estimated timing error is filtered by a first order proportional-integral loop filter. The bandwidth of the filter determines the overall bandwidth of the STR loop, which is usually expressed normalized with respect to the nominal symbol rate. The selection of the loop filter bandwidth is a trade-off between the time needed for the loop to converge (lock-in time) and the loop’s timing-error tracking precision. The filter’s output drives the numerically controlled oscillator (NCO), which is responsible for controlling the time instants of the interpolator output samples. Using these interpolants, the TED will produce its estimate for the next symbol’s timing-error.

Moreover, in steady-state STR loop operation, the loop filter output  $e$  in fact expresses the current relative deviation of the actual symbol rate from the symbol rate during write, namely  $\frac{F-\hat{F}}{F}$ . Based on this estimate and the association between velocity and symbol rate, an estimate of the system’s instant velocity can be extracted as:

$$\hat{v}_{mx} = v_{rx} + B_P N_{TED} F e \quad (5)$$

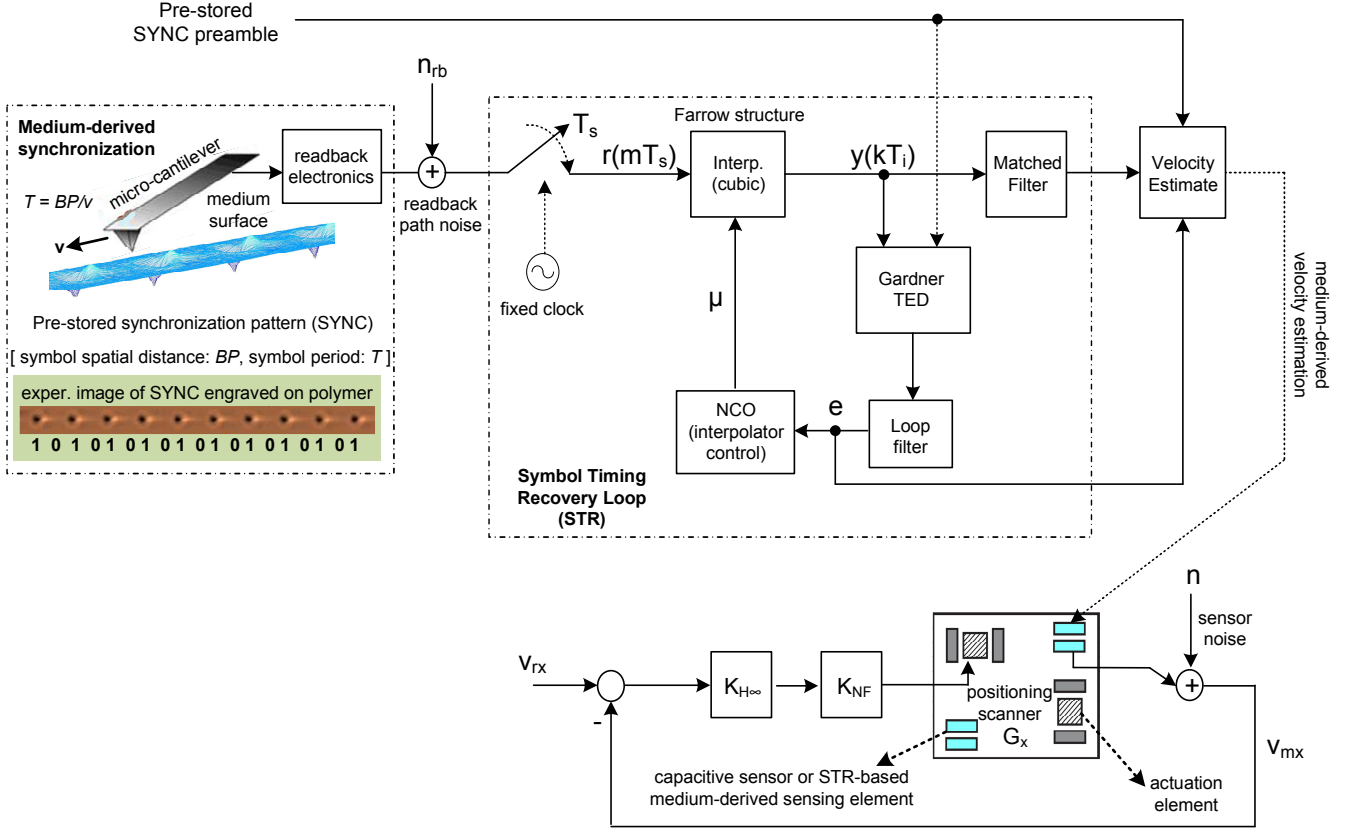


Fig. 3. Block diagram of the overall system architecture.

where  $N_{TED}$  the number of samples per symbol used by the TED. In the Gardner TED case  $N_{TED} = 2$ .

Note that since in this case feedback is provided only by the STR loop, the closed loop system is no longer corrupted by the measurement noise introduced by the position sensors as happens in the standard case. However, the velocity estimate produced by the STR is still noisy. Apart from the non-ideal interpolation process and quantization noise from the analog-to-digital conversion, this is mainly a consequence of storage medium surface inaccuracies of diverse nature, depending on the underlying storage technology. Such inaccuracies are produced during the medium's manufacturing process and corrupt the amplitude of the acquired readback signal. Moreover, it has been shown also experimentally that this type of disturbance presents a near white spectrum in the frequency range of interest [6], [12]. Hence, the combined amplitude noise, denoted by  $n_{rb}$  in Fig. 3, can be well captured by a zero-mean additive white gaussian noise source.

#### IV. PERFORMANCE RESULTS

For the performance evaluation of the proposed architecture, typical operational parameters of probe-based storage systems were chosen, without loss of generality. Specifically, the symbol spatial distance ( $B_p$ ) was set to 10nm and the reference linear velocity ( $v_{xr}$ ) to 0.25nm/ $\mu$ s, yielding a symbol frequency ( $F$ ) of 25kHz. Moreover, the sampling

frequency for the control loop was chosen to be 50kHz, whereas the data sampling frequency  $F_s = 1/T_s$  was fixed at 100 kHz, resulting in an oversampling factor of 4 samples/symbol for the specified  $v_{xr}$  and  $B_p$ . Hence, a downsampling by a factor of 2 was necessary, in order for exactly 2 samples/symbol to be available at the input of the STR loop for proper TED operation. The peak-to-peak amplitude of the synchronization pulses was set to 2nm (0 to 1). Finally, the normalized bandwidth of the STR's first-order loop filter was set to a relatively high value of 0.05 of  $F$  for fast convergence. Note that selecting a lower value would enhance the loop's tracking precision (lower standard deviation of estimated timing error  $e$ ) at the expense of slower convergence speed. For both factors to be improved a two-filter switched scheme can be introduced, so that a high bandwidth filter is used during the acquisition and a lower bandwidth one during the tracking phase. However, such a specialized configuration was outside the scope of this paper.

The efficiency of the STR-based feedback control scheme was assessed in terms of its capability to maintain the selected reference linear velocity of the probe storage system. For this purpose, the standard deviation of the linear velocity was chosen as the appropriate evaluation metric. The proposed system was tested for a wide range of noise levels and was compared with the standard control loop, where the feedback is provided by the integrated position sensor.

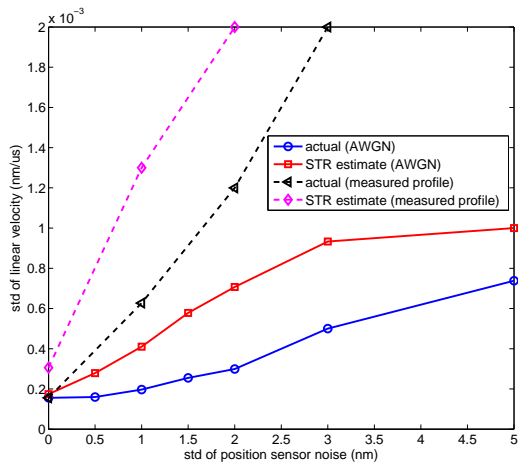


Fig. 6. Effect of position sensor noise on linear velocity's std.

Figures 6 and 7 show how the standard deviation of the actual and estimated linear velocity are affected by the noise level introduced in the closed loop system, for the cases of position sensor feedback (in short Loop-PSF) and STR-based feedback (in short Loop-STR), respectively. In the case where AWG noise is assumed as the sensor noise in Loop-PSF, it is clear from the actual velocity's std in these two figures, that the tracking performance of both loops is similar to the corresponding noise level ranges of interest. This confirms the fact that an STR-based medium-derived feedback architecture can act as an alternative to the standard sensor-based architectures without a degradation in the system's performance. Moreover, the STR-based controller can even provide superior tracking if a different and more realistic noise profile is introduced in the position sensors instead of the AWGN profile. The reason for this is that position sensors of various technologies (such as capacitive, magneto-resistive and thermal sensors) usually present 1/f profiles and/or high spectral components at specific low frequencies (as in our case), to which the low bandwidth closed loop system presented here is more susceptible. Note, that equivalently, the STR-based loop would also perform better in the case of AWG noise but for a high-bandwidth closed loop system with higher susceptibility to the injected measurement noise. As a proof of concept, the measured profile from the x-axis capacitive sensor was used. The corresponding plots are depicted in Fig. 6.

## V. CONCLUSION

A new type of a STR-based tracking controller has been proposed, analyzed and evaluated. It has been shown that such an architecture can be used as an alternative to the standard sensor-based control loop with no performance penalty and with superior performance for certain noise and/or system properties. Furthermore, the existence of an alternative control mechanism enhances the fault-tolerance properties of the overall device in case of sensor unavailability. Finally, the proposed approach robustifies the device's data detection

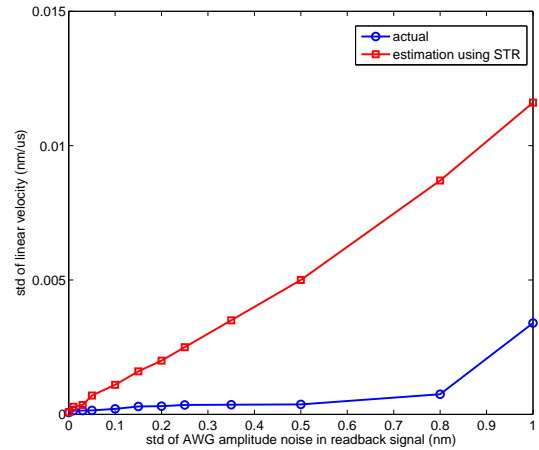


Fig. 7. Effect of readback signal noise on linear velocity's std.

mechanisms against possible storage-medium contractions and expansions stemming from factors and disturbances that are invisible to the standard non-medium-derived control loops.

## REFERENCES

- [1] A. Pantazi, A. Sebastian, T. Antonakopoulos, P. Bächtold, A. R. Bonaccio, J. Bonan, G. Cherubini, M. Despont, R. A. DiPietro, U. Drechsler, U. Dürig, B. Gotsmann, W. Häberle, C. Hagleitner, J. L. Hedrick, D. Jubin, A. Knoll, M. Lantz, J. Pentarakis, H. Posidis, R. C. Pratt, H. Rothuizen, R. Stutz, M. Varsamou, D. Wiesmann, and E. Eleftheriou, "Probe-based ultrahigh-density storage technology," *IBM J. Res. and Dev.*, vol. 52, no. 4/5, pp. 493–511, 2008.
- [2] M. Shibata, H. Yamashita, T. Uchihashi, H. Kandori, and T. Ando, "High-speed atomic force microscopy shows dynamic molecular processes in photoactivated bacteriorhodopsin," *Nature Nanotechnology*, 5, pp. 208–212, 2010.
- [3] S. Mishra, J. Coaplen, and M. Tomizuka, "Precision positioning of wafer scanners," *IEEE Control Systems Magazine*, 27(4), pp. 2025, 2007.
- [4] S. Devasia, E. Eleftheriou, and S. O. R. Moheimani, "A survey of control issues in nanopositioning," *IEEE Trans. on Control System Technology*, vol. 15, no. 5, Sept. 2007.
- [5] A. G. Kotsopoulos and T. A. Antonakopoulos, "Nanopositioning using the spiral of archimedes: The probe-based storage case," *Mechatronics*, vol. 20, no. 2, 2010. [Online]. Available: <http://www.sciencedirect.com/science/article/B6V43-4Y9V88N-1/2/0cf504faed58ac0aec95203b52c5477e>
- [6] H. Pozidis, G. Cherubini, A. Pantazi, A. Sebastian, and E. Eleftheriou, "Channel modeling and signal processing for probe storage channels."
- [7] A. Kotsopoulos, A. Pantazi, A. Sebastian, and T. Antonakopoulos, "High-speed spiral nanopositioning," in *The 18th World Congress of the International Federation of Automatic Control (IFAC)*, Milan, Italy, 2011.
- [8] A. Pantazi, A. Sebastian, G. Cherubini, M. Lantz, H. Pozidis, H. Rothuizen, and E. Eleftheriou, "Control of MEMS-based scanning-probe data storage devices," *IEEE Transactions on Control System Technology*, vol. 15, no. 5, Sept. 2007.
- [9] F. Gardner, "A BPSK/QPSK timing-error detector for sampled receivers," *IEEE Trans. Commun.*, COM-34, pp. 423–429, May 1986.
- [10] F. Gardner, "Interpolation in digital modems-Part I: Fundamentals," *IEEE Transactions on Communications*, vol. 41, no. 3, pp. 501–507, March 1993.
- [11] L. Erup, F. Gardner, and R. Harris, "Interpolation in digital modems-Part II: Implementation and Performance," *IEEE Transactions on Communications*, vol. 41, no. 6, pp. 998–1008, June 1993.
- [12] A. Sebastian, A. Pantazi, H. Pozidis, and E. Eleftheriou, "Nanopositioning for Probe-Based Storage Device," *IEEE Control Systems Magazine*, pp. 26–35, August 2008.